Published October 3, 2005

Rootletin forms centriole-associated filaments and functions in centrosome cohesion

Susanne Bahe,[1] York-Dieter Stierhof,[2] Christopher J. Wilkinson,[1] Florian Leiss,[1] and Erich A. Nigg[1]

[1]Department of Cell Biology, Max-Planck-Institute for Biochemistry, D-82152 Martinsried, Germany
[2]Electron Microscopy Unit, Center for Plant Molecular Biology, University of Tübingen, D-72076 Tübingen, Germany

After duplication of the centriole pair during S phase, the centrosome functions as a single microtubule-organizing center until the onset of mitosis, when the duplicated centrosomes separate for bipolar spindle formation. The mechanisms regulating centrosome cohesion and separation during the cell cycle are not well understood. In this study, we analyze the protein rootletin as a candidate centrosome linker component. As shown by immunoelectron microscopy, endogenous rootletin forms striking fibers emanating from the proximal ends of centrioles. Moreover, rootletin interacts with C-Nap1, a protein previously implicated in centrosome cohesion. Similar to C-Nap1, rootletin is phosphorylated by Nek2 kinase and is displaced from centrosomes at the onset of mitosis. Whereas the overexpression of rootletin results in the formation of extensive fibers, small interfering RNA–mediated depletion of either rootletin or C-Nap1 causes centrosome splitting, suggesting that both proteins contribute to maintaining centrosome cohesion. The ability of rootletin to form centriole-associated fibers suggests a dynamic model for centrosome cohesion based on entangling filaments rather than continuous polymeric linkers.

Introduction

The centrosome is the major microtubule (MT)-organizing center of animal cells (for reviews see Bornens, 2002; Nigg, 2004; Ou and Rattner, 2004; Doxsey et al., 2005). By nucleating and anchoring MTs, it influences most MT-dependent processes, including organelle transport, cell shape, polarity, adhesion, motility, and division. One vertebrate centrosome comprises two centrioles that are embedded in pericentriolar material (PCM). The PCM harbors a large number of proteins with predicted coiled-coil domains (Andersen et al., 2003; for review see Ou and Rattner, 2004). These recruit both γ-tubulin ring complexes for MT nucleation and cell cycle–regulatory proteins (Doxsey et al., 2005). Although substructures have been visualized within the PCM (for review see Ou and Rattner, 2004; Doxsey et al., 2005), the disposition of individual PCM proteins is largely unknown.

After duplication of the two centrioles during S phase (Sluder, 2004), the two resulting centriole doublets continue to function as a single MT-organizing center until they separate at the onset of mitosis. How centrosome cohesion and separation are regulated during the cell cycle is not well understood, but both cytoskeletal dynamics (Euteneuer and Schliwa, 1985; Jean et al., 1999; Thompson et al., 2004) and regulatory protein phosphorylation have been implicated (for review see Meraldi and Nigg, 2001). EM has suggested that centrioles are connected by linker structures (Bornens et al., 1987; Paintrand et al., 1992), but the existence of in vivo linkers remains hypothetical, and their composition is unknown. A 280-kD protein termed C-Nap1 (also known as Cep250; Mack et al., 1998) has been proposed to provide a docking site for a putative linker (Fry et al., 1998a; Mayor et al., 2000). At the onset of mitosis, the inhibition of a type I phosphatase (Helps et al., 2000; Meraldi and Nigg, 2001) is thought to enhance the phosphorylation of C-Nap1 by the protein kinase Nek2 (Fry et al., 1998a; Faragher and Fry, 2003), causing its functional inactivation and, ultimately, its dissociation from the centrosome (Mayor et al., 2000, 2002). To further investigate this model, it would be important to identify proteins that cooperate with C-Nap1 in centrosome cohesion.

Rootletin, a protein distantly related to C-Nap1, was identified as a structural component of the ciliary rootlet in murine photoreceptor cells (Yang et al., 2002) and, independently, in human T lymphoblastoid cells (Andersen et al., 2003).

C.J. Wilkinson's present address is Dept. of Anatomy, University of Cambridge, CB2 3DY Cambridge, UK.

F. Leiss's present address is Dept. of Molecular Neurobiology, Max Planck Institute of Neurobiology, D-82152 Martinsried, Germany.

Correspondence to Erich A. Nigg: nigg@biochem.mpg.de

Abbreviations used in this paper: IF, immunofluorescence; MT, microtubule; PCM, pericentriolar material; siRNA, small interfering RNA.

The online version of this article contains supplemental material.

Supplemental Material can be found at:
http://jcb.rupress.org/content/suppl/2005/10/03/jcb.200504107.DC1.html

The Journal of Cell Biology, Vol. 171, No. 1, October 10, 2005 27–33
http://www.jcb.org/cgi/doi/10.1083/jcb.200504107

Published October 3, 2005

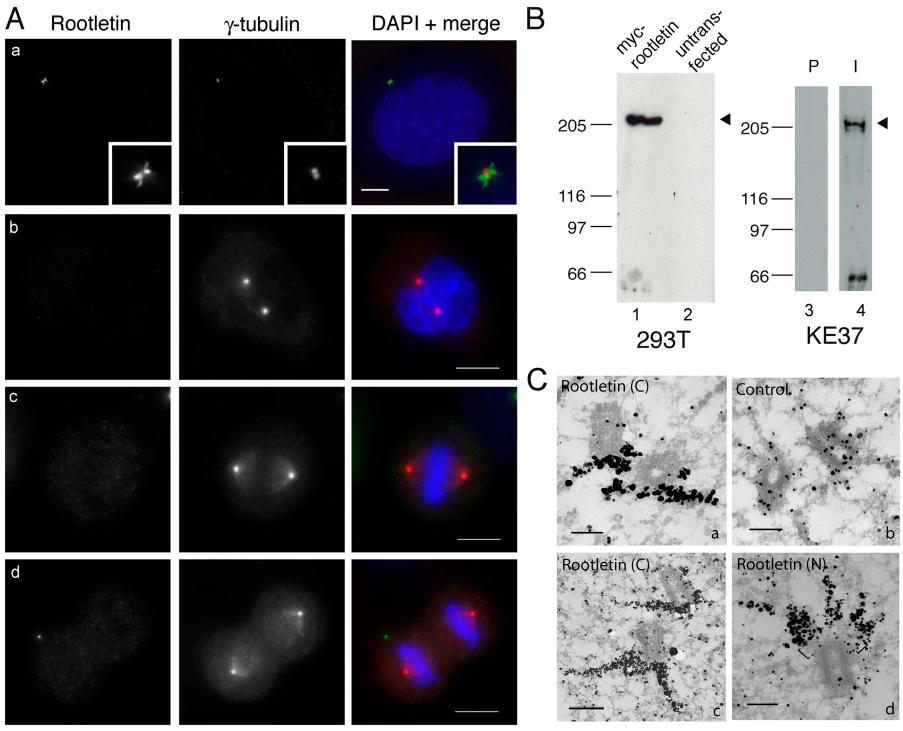

Figure 1. **Human rootletin localizes to centrosomes.** (A) U2OS cells were costained with antirootletin (green) and anti–γ-tubulin (red) antibodies. (a) Interphase cells; insets show enlargements of centrosomes. (b–d) Mitotic cells showing prophase (b), metaphase (c), and telophase (d). DNA was stained with DAPI. Bars, 5 μm. (B) Western blots. (left) Antirootletin antibody R145 on total extracts from myc-rootletin–transfected (lane 1) or untransfected (lane 2) 293T cells. (right) Preimmune (P, lane 3) and antirootletin (I, lane 4) serum on centrosomes isolated from KE37 cells. Arrowheads point to human rootletin. (C) U2OS cells were subjected to preembedding immunogold-labeling EM. Cells were labeled with either antirootletin antibody R145 followed by Nanogold-coupled secondary antibody (a and c), secondary antibody alone (b), or antibodies directed against the NH_2 terminus of rootletin (R146; d). Brackets (d) emphasize the distance of gold particles from the centriole surface with R146 labeling. Bars, 250 nm.

Subsequently, the near complete elimination of rootletin from mice was found to cause photoreceptor degeneration and impaired mucociliary clearance, which is consistent with a key function of this protein in rootlet structures (Yang et al., 2005). In this study, we have explored the hypothesis that rootletin might also be part of an intercentriolar linker structure. Our results confirm that rootletin forms centriole-associated fibrous structures (Yang et al., 2002). Moreover, we show that rootletin interacts functionally with both C-Nap1 and Nek2 kinase. In particular, the depletion of either rootletin or C-Nap1 by small interfering RNA (siRNA) results in centrosome splitting, strongly indicating that both proteins contribute to establishing centrosome cohesion before mitosis.

Results and discussion

Rootletin forms centriole-associated fibers during interphase of the cell cycle

We asked whether rootletin might play a general role in centrosome cohesion. Several antibodies that were raised against recombinant human rootletin recognized a protein of the expected molecular mass (228 kD) in purified centrosomes, whereas the corresponding preimmune serum showed no reactivity (Fig. 1 B). The antibodies also recognized overexpressed rootletin in 293T cells (Fig. 1 B), but no signal representing endogenous rootletin could be detected in any cell line that was tested, including 293T, HeLa S3, and U2OS (Fig. 1 B, Fig. S1 B, available at http://www.jcb.org/cgi/content/full/jcb.200504107/DC1; and not depicted), confirming that rootletin is a low abundance protein in cells that lack a rootlet system (Yang et al., 2002). As shown by immunofluorescence (IF) microscopy, endogenous human rootletin stained thin fibers protruding away from the two centrioles (Fig. 1 A, a). Rootletin staining was uniform throughout interphase, but at least threefold diminished in mitotic cells (Fig. 1 A, b–d). Staining dropped at the onset of prophase (Fig. 1 A, b) and remained low until after telophase (Fig. 1 A, c and d). This suggests that rootletin dissociates from centrosomes as cells go through division, which is highly reminiscent of C-Nap1 (Fry et al., 1998a; Mayor et al., 2000, 2002).

As shown by preembedding immuno-EM, antirootletin antibodies decorated striking fibers emanating from the proximal ends of centrioles (Fig. 1 C, a and c). Proximal ends were identified by the occasional presence of nascent procentrioles next to rootletin fibers (unpublished data). Often, two to four rootletin-positive fibers emanated from individual centrioles, with the length of some fibers exceeding 0.5 μm. Antirootletin antibodies directed against the COOH or NH_2 terminus produced qualitatively similar results, but the epitopes recognized by the former antibody were closer to the centriolar surface (Fig. 1 C, compare a and c with d), suggesting that rootletin fibers attach to centrioles via their COOH termini. Controls showed background labeling but no labeled fibers (Fig. 1 C, b). These results indicate that rootletin does not provide a continuous linker between centrioles but do not exclude a role in centrosome cohesion.

Rootletin interacts with C-Nap1 and Nek2

We next sought to determine whether rootletin was able to interact with C-Nap1 and/or Nek2, which are two proteins that were previously implicated in centrosome cohesion (Fry et al., 1998a; Mayor et al., 2000, 2002). Endogenous C-Nap1 localizes to the proximal ends of centrioles, suggesting that it might constitute docking sites for rootletin fibers, whereas Nek2 has

Published October 3, 2005

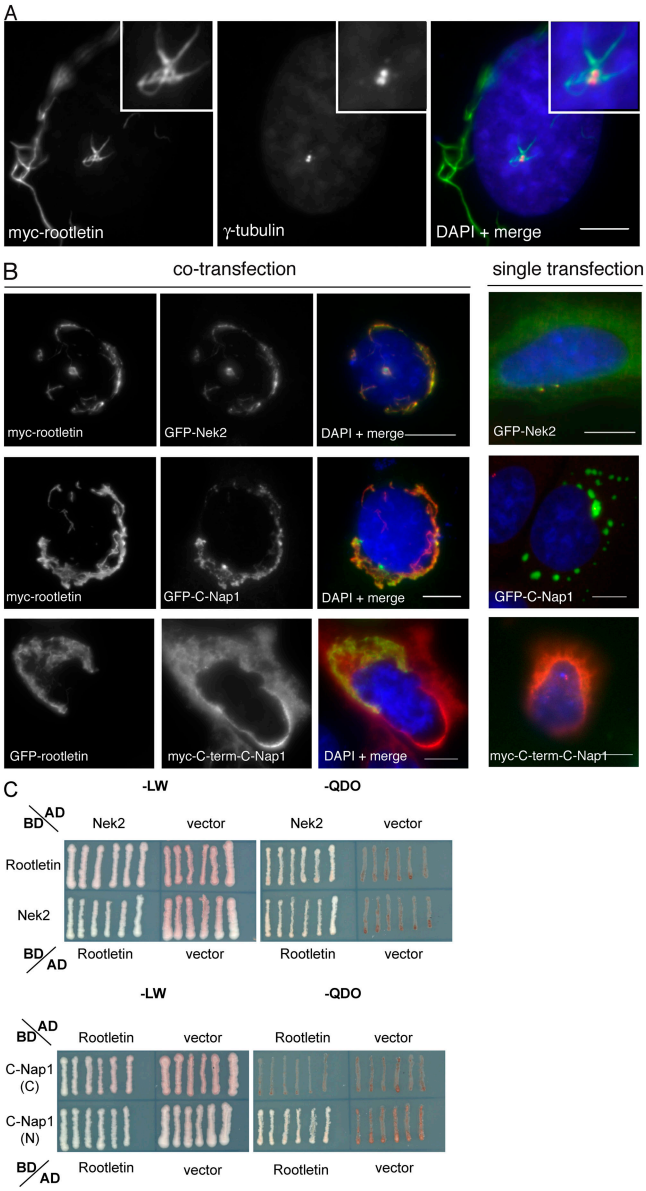

Figure 2. **Rootletin interacts with itself, C-Nap1, and Nek2.** (A) U2OS cells were transfected with myc-tagged rootletin (green) and were counterstained with anti–γ-tubulin antibody (red). Insets show enlargements of the centrosomes to highlight protein fibers. Bar, 5 μm. (B) U2OS cells were transfected with tagged Nek2, C-Nap1, or a COOH-terminal fragment of C-Nap1 either alone (right) or together with rootletin (left three panels), and the distribution of proteins was monitored by IF microscopy. Bars, 15 μm. (C) Yeast two-hybrid interaction of rootletin with Nek2 (top) and C-Nap1 (bottom). Transformed yeast cells were plated onto media selecting for transformants (−LW) and bait-prey interactions (−QDO), respectively. AD, activation domain; BD, binding domain; LW, leucine tryptophane; QDO, quadruple drop out.

been implicated in the regulation of C-Nap1. As a result of the low abundance of rootletin and our inability to detect endogenous rootletin by any of the available antibodies, coimmunoprecipitation experiments were not successful. Thus, we asked whether rootletin is able to interact with C-Nap1 and/or Nek2 upon coexpression in U2OS cells. The overexpression of rootletin alone led to the formation of striking filaments (Fig. 2 A), which is consistent with earlier data (Yang et al., 2002). These filaments emanated from the centrosome at low expression levels (Fig. 2 A) but filled the cytoplasm at higher levels (Fig. 2 B). The expression of GFP-Nek2 or GFP–C-Nap1 alone resulted in a diffuse distribution or in the formation of multiple globular aggregates, respectively (Fig. 2 B), as described previously (Fry et al., 1998b; Mayor et al., 2002). In stark contrast, the coexpression of either GFP-Nek2 or GFP–C-Nap1 with rootletin resulted in their recruitment to rootletin filaments (Fig. 2 B). Several proteins encompassing COOH-terminal domains of C-Nap1 were not recruited, nor was GFP–centrin-2 (Fig. 2 B and not depicted). This latter result not only provides a specificity control but also indicates that rootletin binding requires the NH_2 terminus of C-Nap1.

To confirm that rootletin is able to interact with Nek2 and C-Nap1, we performed yeast two-hybrid experiments (Fig. 2 C). Rootletin interacted with Nek2 (Fig. 2 C, top) and with itself (not depicted; Yang et al., 2002). Moreover, it bound an NH_2-terminal but not a COOH-terminal fragment of C-Nap1 (Fig. 2 C, bottom), which is in line with the aforementioned results (Fig. 2 B).

C-Nap1 was identified as a substrate of Nek2 (Fry et al., 1998a). To determine whether rootletin might also be regulated by Nek2, we transfected U2OS cells with wild-type or catalytically inactive Nek2 and monitored the localization of endogenous rootletin by IF microscopy. Whereas the overexpression of inactive Nek2 did not detectably affect rootletin localization, wild-type kinase caused the dissociation of rootletin from centrosomes (Fig. 3 A). In addition, wild-type Nek2 caused centrosome splitting as expected (Fry et al., 1998b). Active Nek2, but not the catalytically inactive mutant, also retarded the mobility of rootletin (Fig. 3 B). This mobility shift was sensitive to phosphatase treatment (unpublished data), indicating that rootletin was phosphorylated by Nek2 either directly or indirectly. When different rootletin fragments (Fig. 3 C) were coexpressed with active Nek2, they were all upshifted (Fig. 3 D), suggesting the existence of multiple phosphorylation sites. To determine whether rootletin was a direct substrate of Nek2, in vitro kinase assays were performed. Upon the incubation of NH_2- and COOH-terminal fragments with Nek2 in the presence of γ-[^{32}P]ATP, both were readily phosphorylated by active but not inactive Nek2 (Fig. 3 E), which is consistent with the aforementioned results. All samples containing active Nek2 showed an additional phosphorylated band at ∼50 kD (Fig. 3 E), reflecting autophosphorylation (Fry et al., 1995).

An attractive model holds that centrosome cohesion is regulated by a balance of kinase and phosphatase activities (Fry et al., 1998b; Helps et al., 2000; Meraldi and Nigg, 2001). Therefore, we examined the fate of rootletin after interfering with cellular phosphatase activity. Inhibition of type 1 and type 2A phosphatases in hTERT-RPE1 and U2OS cells by calyculin A resulted in centrosome splitting (Fig. S1 and not depicted) and in the concomitant loss of rootletin from split centrosomes (Fig. S1). Interestingly, rootletin dissociation could be observed even before a significant loss of C-Nap1 was apparent (Fig. S1). These results support the hypothesis that the association of rootletin with centrosomes is regulated by phosphorylation.

Published October 3, 2005

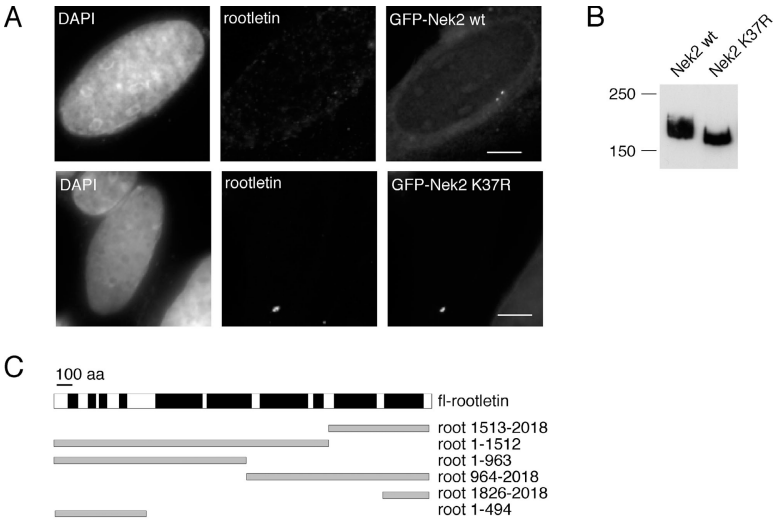

Figure 3. **Nek2 phosphorylates rootletin.** (A) U2OS cells were transfected with wild-type (wt) or catalytically inactive (K37R) GFP-Nek2, and endogenous rootletin was stained with antibody. Bars, 5 μm. (B–D) After the coexpression of GFP-Nek2 with full-length myc-rootletin (B) or myc-rootletin fragments (D, arrowheads), total 293T cell extracts were probed by Western blotting with anti-myc antibody. (C) Schematic illustrating rootletin fragments (black bars indicate predicted coiled-coil). (E) In vitro kinase assay using wild-type or K37R Nek2 on His-rootletin NH_2- and COOH-terminal fragments. Proteins were resolved by SDS-PAGE, and gels were subjected to autoradiography (left) and Coomassie blue staining (right). Arrowheads indicate the migration of His-rootletin fragments; the arrow points to autophosphorylated Nek2.

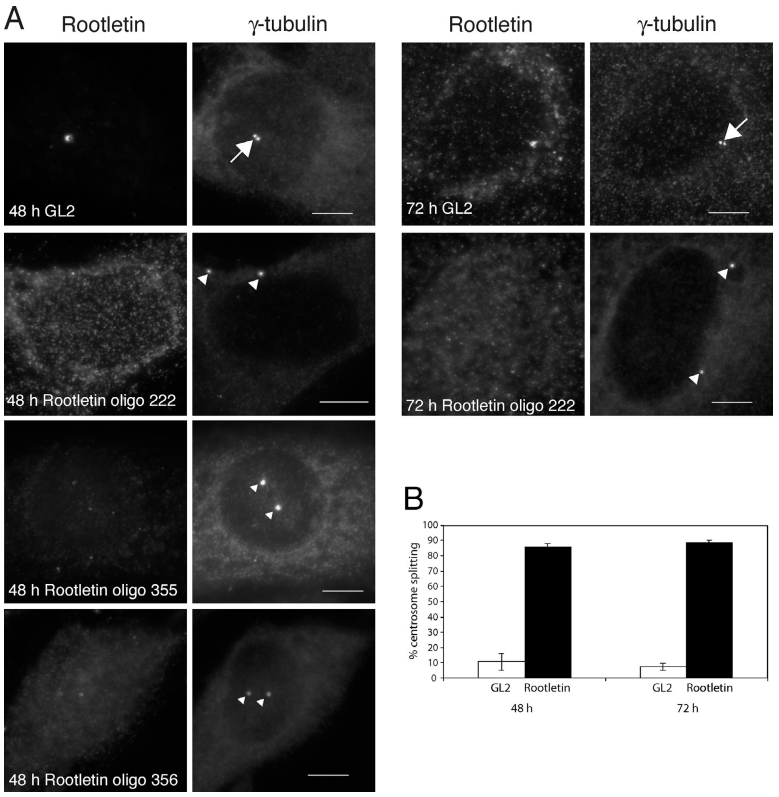

Figure 4. **siRNA depletion of rootletin causes centrosome splitting.** (A) U2OS cells were transfected for 48 or 72 h with control (GL2) or different rootletin-specific siRNA duplexes and were costained for rootletin and γ-tubulin. Arrows and arrowheads mark paired centrioles and split centrosomes, respectively. Bars, 10 μm. (B) Quantitation of centrosome splitting in control (GL2) or rootletin siRNA-treated cells (oligonucleotide 222). Centrosomes were counted as split when the distance between centrioles was >2 μm. Error bars represent SEM.

Published October 3, 2005

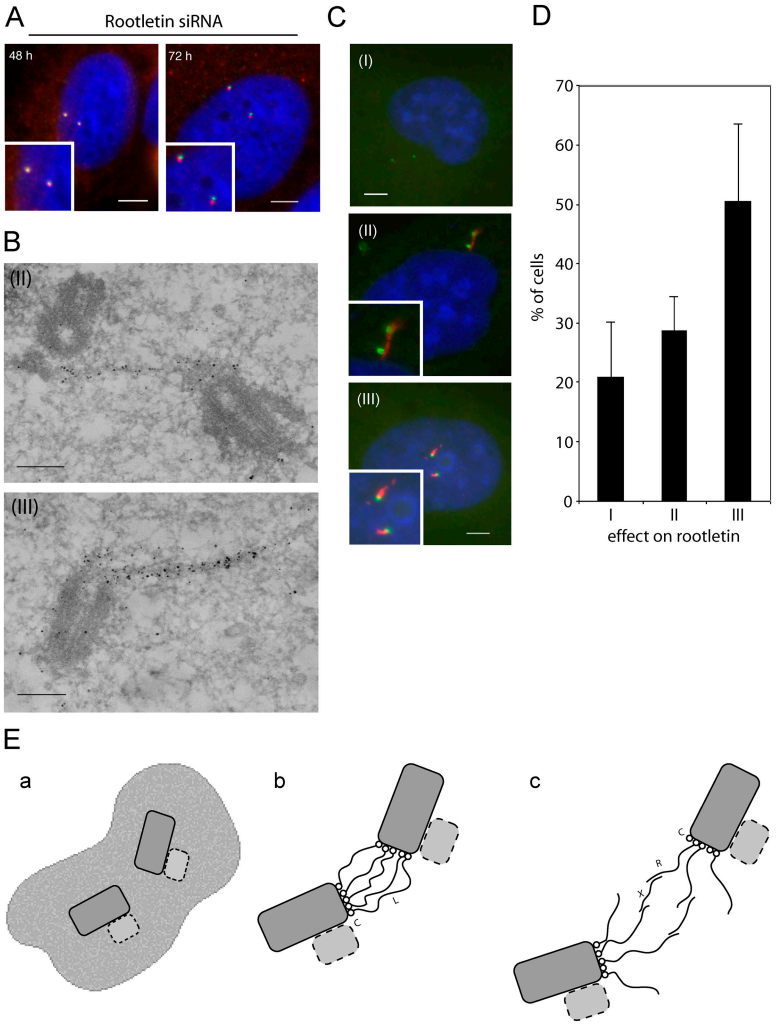

Figure 5. **Mutual dependency of rootletin and C-Nap1 localization and models for centrosome cohesion.** (A) U2OS cells were transfected for 48 or 72 h with control (GL2) or rootletin-specific siRNA duplexes and were stained for C-Nap1 (green) and γ-tubulin (red). Bars, 5 μm. (B) U2OS cells were depleted of C-Nap1 by siRNA and were subjected to immuno-EM labeling of rootletin (antibody R145). Bars, 250 nm. (C) U2OS cells were transfected for 48 h with a C-Nap1–specific siRNA duplex and were stained for rootletin (red) and γ-tubulin (green). Rootletin disappeared altogether (I) and formed elongated fibers that either appeared to connect split centrosomes (II) or protruded away from split centrosomes (III). Bars, 5 μm. (A and C) Insets show enlargements of the centrosome area to highlight centrosome splitting. (D) Quantitation of the observed effects of C-Nap1 RNA interference on rootletin localization (I–III; compare with C). Error bars represent SEM. (E) Schematic illustration of possible models for centrosome cohesion. (a) Centrioles (rectangles) embedded in the PCM (speckled). (b) Centrioles connected by a continuous proteinaceous linker. (c) Centrioles connected by entangling filaments. C, C-Nap1; L, hypothetical continuous linker; R, rootletin; X, additional linker proteins that are yet to be identified. Parental centrioles (dark gray) are depicted as having associated nascent procentrioles (dotted lines).

siRNA-mediated depletion of rootletin causes centrosome splitting

To test more directly whether rootletin was involved in centrosome cohesion, we used siRNA. Three different rootletin-specific duplex oligonucleotides caused the near complete loss of rootletin from the centrosome (Fig. 4 A) and, concomitantly, extensive centrosome splitting (Fig. 4). In quantitative terms, >85% of cells that were treated with the most efficient siRNA duplex displayed split centrosomes, whereas <11% of cells showed a similar phenotype in GL2 control–treated cells (Fig. 4 B). Rootletin depletion caused centrosome splitting not only in U2OS but also in hTERT-RPE1 and A549 cells (Fig. S2, available at http://www.jcb.org/cgi/content/full/jcb.200504107/DC1). Centrosome splitting was observed upon the siRNA-mediated depletion of C-Nap1 (Fig. S3, available at http://www.jcb.org/cgi/content/full/jcb.200504107/DC1), which is a protein that was previously implicated in centrosome cohesion (Mayor et al., 2000), but not upon the depletion of Cep170, centrin-2, BBS4, PCM-1, or ninein. These results indicate that centrosome splitting is not a general response to the depletion of centrosomal proteins, supporting the hypothesis that both rootletin and C-Nap1 contribute to confer centrosome cohesion. Additional proteins that are involved in this process certainly await identification, as indicated by the recent demonstration that the depletion of dynamin-2 also causes centrosome splitting (Thompson et al., 2004).

We next asked whether the depletion of rootletin would impair the localization of C-Nap1 or vice versa. The depletion of rootletin did not detectably influence the association of C-Nap1 with centrosomes (Fig. 5 A), but the depletion of C-Nap1 clearly affected the localization of rootletin (Fig. 5, B and C). In siRNA experiments targeting C-Nap1, the protein was completely depleted in ∼20% of cells and was strongly depleted in the remainder (unpublished data). In line with this observation, rootletin was no longer detectable at centrosomes in 21% of C-Nap1–depleted cells (Fig. 5, C and D, I). In the other cells, rootletin could be seen to form fibers (Fig. 5 C, II and III) that were fewer and often more than twice as long as those seen in control cells (Fig. 1 A). These fibers either pointed in various directions (50% of cells; Fig. 5, C and D, III) or appeared to span the entire distance between the two parental centrioles (29% of cells; Fig. 5, C and D, II). The observation that rootletin was not lost from all centrioles upon C-Nap1 depletion probably reflects residual levels of C-Nap1, although interactions with other centriolar proteins cannot be excluded. If one assumes that C-Nap1 docking sites and preexisting rootletin fi-

Published October 3, 2005

bers compete for the binding of rootletin subunits, a reduced number of docking sites would be expected to result in the anchoring of fewer but longer rootletin fibers exactly as seen in Fig. 5 (B and C).

Altogether, the aforementioned data indicate that rootletin cooperates with C-Nap1 to establish centrosome cohesion and that both proteins are regulated by phosphorylation during the cell cycle. These findings have implications for different models of centrosome cohesion (Fig. 5 E). In principle, centrosome cohesion might result from the embedding of centrioles in a matrix composed of PCM proteins (Fig. 5 E, a). In this scenario, rootletin could contribute to the anchoring of centrioles to an underlying matrix. Alternatively, it is possible that cohesion is established by specialized linker proteins, as illustrated in Fig. 5 E (b and c). All of these models need to accommodate the fact that, at least in some cells, the two centrioles of the original diplosome become widely separated already during G1 (Sherline and Mascardo, 1982; Euteneuer and Schliwa, 1985; Whitehead et al., 1996) and that centrioles display a striking mobility (Piel et al., 2000). With regard to the second model in Fig. 5 E (b), this implies that any linker would have to be extremely flexible and variable in length. Proteins spanning the entire distance between parental centrioles may await discovery, but the localization of rootletin does not fit a continuous linker model. Instead, the results reported in this study prompt us to favor the third model (Fig. 5 E, c). Specifically, we postulate that centrosome cohesion results from the entangling of filaments that are associated with both parental centrioles. If rootletin fibers were to interact with additional bridging proteins, this would provide for a highly dynamic linker structure of variable dimensions. Compared with continuous intercentriolar connections (Fig. 5 E, b), centriole–centriole interactions that are based on entangling filaments (Fig. 5 E, c) would readily allow for occasional linker disruption and major variations in linker length between different cell types or cell cycle stages. Conversely, such a mechanism could explain why centrioles eventually formed de novo aggregate without being connected from the start (La Terra et al., 2005). Thus, the third model (Fig. 5 E, c) seems to best accommodate the available information on centriole dynamics, the regulation of centrosome cohesion by phosphorylation, and the properties of C-Nap1 and rootletin. While awaiting further validation, this working model will hopefully provide a useful framework for continued studies on the mechanisms underlying centrosome cohesion and separation.

Materials and methods

Plasmid preparation and recombinant proteins

The partial cDNA clones KIAA0445 (Kazusa DNA Research Institute) and IMAGE clone 6150861 (Deutsches Ressourcenzentrum fuer Genomforschung GmbH) were fused, and the complete coding sequence for rootletin was subcloned into pEGFP-C1 (CLONTECH Laboratories, Inc.). A plasmid encoding myc-rootletin was prepared by replacing the GFP tag, and the myc-tagged deletion mutant root 1–963 (aa 1–963) was prepared by excision of the corresponding COOH-terminal sequence. Roots 1–1512 (aa 1–1512), 964–2018 (aa 964–2018), and 1513–2018 were produced in pcDNA3.1/3× myc-B/-C (Invitrogen). For the expression of recombinant rootletin fragments, roots 1826–2018 and 1–494 were PCR amplified and inserted into the expression vector pET28b+ (Novagene). His_6-tagged rootletin fragments were expressed in *Escherichia coli* strain BL21(DE3) and purified under denaturing conditions by using standard protocols (QIAexpressionist system; QIAGEN). All constructs were confirmed by sequencing.

Antibody production

Antirootletin pAbs were raised against roots 1826–2018 (R145) and 1–494 (R146/R147; Charles River Laboratories). Antibodies against C-Nap1 have been described previously (R63; Fry et al., 1998a).

Cell culture, transfections, and Western blotting

hTERT-RPE1cells were provided by A. Mikhailov (Wadsworth Center, Albany, NY). Cells were grown at 37°C under 5% CO_2 in DME supplemented with 10% FCS and penicillin-streptomycin (100 IU/ml and 100 μg/ml, respectively). 293T cells were transfected by using the calcium phosphate precipitation method. U2OS and HeLaS3 cells were transfected by using Fugene6 reagent (Roche) according to the manufacturer's protocol. For immunoblotting experiments, which were performed as described previously (Fry et al., 1998a), primary antibodies were used at the following concentrations: rabbit antirootletin serum or corresponding preimmune serum (R145; 1:1,000), mAb anti-myc (9E10; 1:3), and rabbit anti–C-Nap1 affinity-purified IgG (R63; gift from T. Mayor, California Institute of Technology, Pasadena, CA; Mayor et al., 2000). Secondary antibodies were HRP-conjugated goat anti–rabbit (1:7,000; Bio-Rad Laboratories) or anti–mouse (1:3,000; Bio-Rad Laboratories) IgGs. Calyculin A treatments to induce centrosome splitting were performed as described previously (Meraldi and Nigg, 2001).

IF microscopy

Cells for IF were fixed, stained, mounted, and observed as described previously by Meraldi and Nigg (2001). Primary antibodies were rabbit antirootletin serum (R145; 1:1,000), mouse anti–γ-tubulin mAb (1:1,000; GTU-88; Sigma-Aldrich), and rabbit anti–C-Nap1 affinity-purified IgG (R63; Mayor et al., 2000). Secondary antibodies were AlexaFluor488- and AlexaFluor555-conjugated donkey anti–mouse and anti–rabbit IgGs (1:1,000; Invitrogen).

For high resolution images, a microscope (Deltavision; Applied Precision) on a base (Nikon Eclipse TE200; Applied Precision) that was equipped with S Fluor 40×/1.3 and Plan Apo 60×/1.4 oil immersion objectives (Nikon) and a camera (CoolSNAP HQ; Photometrics) was used for collecting 0.15- and 0.2-μm–distanced optical sections in the z-axis for pictures of interphase and mitotic cells, respectively. Immersion oil (n = 1.512) was used at 18°C. For Figs. 1 A and 2 A, images at single focal planes were processed with a deconvolution algorithm, and optical sections were projected into one picture using the Softworx software (Applied Precision). All other Deltavision images were processed the same way but without deconvolution. Exposure times were set such that the camera response was in the linear range for each fluorophor. Images were cropped in Adobe Photoshop 5.5/6.0 and were sized and placed in figures using Adobe Illustrator 8.0/11.0 (Adobe Systems, Inc.).

Immuno-EM

For the preembedding immuno-EM of whole cells, U2OS cells that were grown on coverslips were fixed with 4% PFA for 10 min and were permeabilized with PBS + 0.5% Triton X-100 for 2 min. Blocking and primary antibody incubations were performed as described for IF microscopy followed by incubation with goat anti–rabbit IgG Nanogold (1:50–1:100; Nanoprobes). Nanogold was silver enhanced with HQ Silver (Nanoprobes). The primary antibody was omitted for controls. Cells were further processed as described previously (Fry et al., 1998a).

Yeast two-hybrid experiments

The entire coding sequence of human rootletin cDNA was inserted into the two-hybrid prey vector pACT2 (CLONTECH Laboratories, Inc.) and the bait vector pFBT9 (a version of pGBT9; CLONTECH Laboratories, Inc.; modified to encode kanamycin resistance, which was a gift from F. Barr, Max-Planck-Institute for Biochemistry, Martinsried, Germany). These plasmids were cotransformed with plasmids encoding full-length Nek2 and NH_2- and COOH-terminal deletion mutants of C-Nap1 (aa 1–647 and 1852–2442, respectively) into the yeast strain PJ69-4A. Transformed yeasts were plated onto media lacking either leucine and tryptophane (−LW) or media lacking leucine, tryptophan, histidine, and adenine with 2% (wt/vol) glucose as the carbon source (quadruple drop out [−QDO]). All results were confirmed by streaking six independent colonies onto both selective (−QDO) and nonselective (−LW) plates and scoring growth after 2 d at 30°C.

Published October 3, 2005

Nek2 kinase assay

In vitro kinase assays with recombinant His_6-tagged rootletin fragments were performed in kinase buffer (50 mM Hepes-KOH, pH 7.4, 5 mM $MnCl_2$, 5 mM β-glycerophosphate, 5 mM NaF, 1 μM okadaic acid, 1 mM DTT, 1 mM PMSF, 10 μg/ml leupeptin, 10 μg/ml aprotinin, and 10 μg/ml pepstatin A) containing 500 μM ATP, 1 μCi γ-[^{32}P]ATP (3,000 Ci/mmol and 10 mCi/ml; GE Healthcare), and substrate at 500 μg/ml. Equal amounts of recombinant proteins or casein for control were used with wild-type or catalytically inactive (K37R) Nek2 (Fry et al., 1995). Nek2 was immunopurified from baculovirus-infected Sf9 insect cells as described previously (Fry et al., 1995). Incubation was performed for 30 min at 30°C, and reactions were stopped by adding 5× gel sample buffer and boiling for 5 min. Samples were electrophoresed, and phosphate incorporation was determined by autoradiography.

siRNA experiments

Rootletin was depleted by using 20 μM siRNA duplex oligonucleotides targeting the following sequences: 5′-AAGCCAGTCTAGACAAGGA-3′ (oligonucleotide 222; Dharmacon), 5′-CAGGGAGATTGTCACCCGCAA-3′ (oligonucleotide 355; QIAGEN), and 5′-CAGCCAGGAGAAGAT-CAGCAA-3′ (oligonucleotide 356; QIAGEN). Duplexes that were used for the depletion of C-Nap1 were 5′-CTGGAAGAGCGTCTAACTGAT-3′ (oligonucleotide 239; QIAGEN) and 5′-GCGGAGCTCTCTGAAGTTAAA-3′ (oligonucleotide 299; QIAGEN) for ninein. The siRNA duplexes that were used for the efficient depletion of other proteins have previously been validated: centrin-2 (5′-AAGAGCAAAAGCAGGAGATCC-3′), Cep170 (5′-GAAGGAATCCTCCAAGTCA-3′), BBS4 (5′-AAGGCACAA-GACCAGTTGCAC-3′), and PCM-1 (5′-AATCAGCTTCGTGATTCTCAG-3′). Transfections were performed as described previously using the oligo-duplex GL2 for control (Elbashir et al., 2001).

Centrosome preparations

Human centrosomes were isolated from KE37 cells as described previously (Andersen et al., 2003).

Online supplemental material

Fig. S1 shows that calyculin A–induced centrosome splitting displaces rootletin from centrosomes. Fig. S2 shows centrosome splitting by rootletin depletion in different cell lines, and Fig. S3 shows the siRNA-mediated depletion of C-Nap1. Online supplemental material is available at http://www.jcb.org/cgi/content/full/jcb.200504107/DC1.

We thank A. Mikhailov for providing hTERT-RPE1 cells, F. Barr and T. Mayor for providing reagents, and X. Yan and R. Habedanck for helpful discussions.

This work was supported by the Max-Planck-Society, the Deutsche Forschungsgemeinschaft (grant SFB413), and the Fonds der Chemischen Industrie.

Submitted: 19 April 2005
Accepted: 2 September 2005

References

Andersen, J.S., C.J. Wilkinson, T. Mayor, P. Mortensen, E.A. Nigg, and M. Mann. 2003. Proteomic characterization of the human centrosome by protein correlation profiling. *Nature.* 426:570–574.

Bornens, M. 2002. Centrosome composition and microtubule anchoring mechanisms. *Curr. Opin. Cell Biol.* 14:25–34.

Bornens, M., M. Paintrand, J. Berges, M.C. Marty, and E. Karsenti. 1987. Structural and chemical characterization of isolated centrosomes. *Cell Motil. Cytoskeleton.* 8:238–249.

Doxsey, S., D. McCollum, and W. Theurkauf. 2005. Centrosomes in cellular regulation. *Annu. Rev. Cell Dev. Biol.* 10.1146/annurev.cellbio.21.122303.120418.

Elbashir, S.M., J. Harborth, W. Lendeckel, A. Yalcin, K. Weber, and T. Tuschl. 2001. Duplexes of 21-nucleotide RNAs mediate RNA interference in cultured mammalian cells. *Nature.* 411:494–498.

Euteneuer, U., and M. Schliwa. 1985. Evidence for an involvement of actin in the positioning and motility of centrosomes. *J. Cell Biol.* 101:96–103.

Faragher, A.J., and A.M. Fry. 2003. Nek2A kinase stimulates centrosome disjunction and is required for formation of bipolar mitotic spindles. *Mol. Biol. Cell.* 14:2876–2889.

Fry, A.M., S.J. Schultz, J. Bartek, and E.A. Nigg. 1995. Substrate specificity and cell cycle regulation of the Nek2 protein kinase, a potential human homolog of the mitotic regulator NIMA of *Aspergillus nidulans*. *J. Biol. Chem.* 270:12899–12905.

Fry, A.M., T. Mayor, P. Meraldi, Y.D. Stierhof, K. Tanaka, and E.A. Nigg. 1998a. C-Nap1, a novel centrosomal coiled-coil protein and candidate substrate of the cell cycle-regulated protein kinase Nek2 105. *J. Cell Biol.* 141:1563–1574.

Fry, A.M., P. Meraldi, and E.A. Nigg. 1998b. A centrosomal function for the human Nek2 protein kinase, a member of the NIMA family of cell cycle regulators. *EMBO J.* 17:470–481.

Helps, N.R., X. Luo, H.M. Barker, and P.T. Cohen. 2000. NIMA-related kinase 2 (Nek2), a cell-cycle-regulated protein kinase localized to centrosomes, is complexed to protein phosphatase 1. *Biochem. J.* 349:509–518.

Jean, C., Y. Tollon, B. Raynaud-Messina, and M. Wright. 1999. The mammalian interphase centrosome: two independent units maintained together by the dynamics of the microtubule cytoskeleton. *Eur. J. Cell Biol.* 78:549–560.

La Terra, S., C.N. English, P. Hergert, B.F. McEwen, G. Sluder, and A. Khodjakov. 2005. The de novo centriole assembly pathway in HeLa cells: cell cycle progression and centriole assembly/maturation. *J. Cell Biol.* 168:713–722.

Mack, G.J., J. Rees, O. Sandblom, R. Balczon, M.J. Fritzler, and J.B. Rattner. 1998. Autoantibodies to a group of centrosomal proteins in human autoimmune sera reactive with the centrosome. *Arthritis Rheum.* 41:551–558.

Mayor, T., Y.D. Stierhof, K. Tanaka, A.M. Fry, and E.A. Nigg. 2000. The centrosomal protein C-Nap1 is required for cell cycle-regulated centrosome cohesion. *J. Cell Biol.* 151:837–846.

Mayor, T., U. Hacker, Y.D. Stierhof, and E.A. Nigg. 2002. The mechanism regulating the dissociation of the centrosomal protein C-Nap1 from mitotic spindle poles. *J. Cell Sci.* 115:3275–3284.

Meraldi, P., and E.A. Nigg. 2001. Centrosome cohesion is regulated by a balance of kinase and phosphatase activities. *J. Cell Sci.* 114:3749–3757.

Nigg, E.A. 2004. Centrosomes in Development and Disease. Wiley-VCH, Weinheim. 431 pp.

Ou, Y., and J.B. Rattner. 2004. The centrosome in higher organisms: structure, composition, and duplication. *Int. Rev Cytol.* 238:119–182.

Paintrand, M., M. Moudjou, H. Delacroix, and M. Bornens. 1992. Centrosome organization and centriole architecture: their sensitivity to divalent cations. *J. Struct. Biol.* 108:107–128.

Piel, M., P. Meyer, A. Khodjakov, C.L. Rieder, and M. Bornens. 2000. The respective contributions of the mother and daughter centrioles to centrosome activity and behavior in vertebrate cells. *J. Cell Biol.* 149:317–330.

Sherline, P., and R. Mascardo. 1982. Epidermal growth factor-induced centrosomal separation: mechanism and relationship to mitogenesis. *J. Cell Biol.* 95:316–322.

Sluder, G. 2004. Centrosome duplication and its regulation in the higher animal cell. *In* Centrosomes in Development and Disease. E.A. Nigg, editor. Wiley-VCH, Weinheim. 167–189.

Thompson, H.M., H. Cao, J. Chen, U. Euteneuer, and M.A. McNiven. 2004. Dynamin 2 binds gamma-tubulin and participates in centrosome cohesion. *Nat. Cell Biol.* 6:335–342.

Whitehead, C.M., R.J. Winkfein, and J.B. Rattner. 1996. The relationship of HsEg5 and the actin cytoskeleton to centrosome separation. *Cell Motil. Cytoskeleton.* 35:298–308.

Yang, J., X. Liu, G. Yue, M. Adamian, O. Bulgakov, and T. Li. 2002. Rootletin, a novel coiled-coil protein, is a structural component of the ciliary rootlet. *J. Cell Biol.* 159:431–440.

Yang, J., J. Gao, M. Adamian, X.H. Wen, B. Pawlyk, L. Zhang, M.J. Sanderson, J. Zuo, C.L. Makino, and T. Li. 2005. The ciliary rootlet maintains long-term stability of sensory cilia. *Mol. Cell. Biol.* 25:4129–4137.